



J. Chem. Pharm. Res., 2010, 2(4):835-850

ISSN No: 0975-7384
CODEN(USA): JCPRC5

Comparative conformational, structural and vibrational study on the molecular structure of tyrosine and L-DOPA using density functional theory

**Shamoon Ahmad Siddiqui¹, Anoop Kumar Pandey², Apoorva Dwivedi², Sudha Jain³,
Neeraj Misra^{2*}**

¹*Shri Ramswaroop Memorial College of Engg. and Management, Lucknow, India*

²*Department of Physics, Lucknow University, Lucknow, India*

³*Department of Chemistry, Lucknow University, Lucknow, India*

ABSTRACT

A brief conformational, structural and vibrational study has been performed on the molecular structure of two well known amino acids tyrosine and L-DOPA. The equilibrium geometry, harmonic vibrational frequencies, infrared intensities and Raman scattering activities were calculated by the Density Functional B3LYP method employing 6-311G(d,p) as the basis set and the vibrational studies were interpreted in terms of potential energy distribution (P.E.D.). The internal coordinates were optimized repeatedly to maximize the P.E.D. contributions. A detailed interpretation of the infrared and Raman spectra of tyrosine and L-DOPA is reported in the present work. The similarities and differences between the vibrational spectra of the two molecules studied have been highlighted. The calculations are in agreement with experiment. The thermodynamic calculations related to the title compounds were also performed at B3LYP/6-311G(d,p) level of theory. The FT-Raman and FT-IR spectra of tyrosine and L-DOPA have been taken from literature.

Keywords: FT-IR and FT-Raman Spectra; Density functional theory; P.E.D.; Tyrosine and L-DOPA; Vibrational study.

INTRODUCTION

Tyrosine (4-hydroxyphenylalanine) also known as L-tyrosine is a non essential amino acid that is a building block of protein. It is a precursor of the neurotransmitter dopamine, as well as a

precursor to the adrenal hormones norepinephrine and epinephrine. The body can make tyrosine from the amino acid phenylalanine [1]. We get tyrosine in our body by eating protein-rich foods like meat, fish, eggs, dairy products and beans. Tyrosine is used by the body to make the neurotransmitter noradrenaline. Noradrenaline is believed to be in short supply in the brains of people who are depressed [2]. Tyrosine may help athletes avoid overtraining, due to its ability to offset fatigue [3]. Because tyrosine is a precursor of dopamine, supplementing with tyrosine may heighten mental alertness, increase feeling of well being, decrease feelings of depression, and offset physical and mental fatigue [4,5]. Tyrosine also serves to protect the integrity of the skin. Melanin, a substance which acts to protect the skin when the epidermis has been exposed to ultraviolet light, is derived from tyrosine. If a shortage of melanin is present within the body, skin defenses will be compromised. Melanin, which is derived from tyrosine, chemically reacts with sunlight to form a protective shield that protects the deeper layers of skin tissue [6]. People suffering from neurological degeneracy may also benefit from supplemental tyrosine [7]. The conversion of tyrosine to L-DOPA is catalyzed by tyrosine hydroxylase (TyrOH). TyrOH is a non-heme iron enzyme which uses molecular oxygen to hydroxylate tyrosine to form L-dihydroxyphenylalanine (L-DOPA) [8,9].

Levodopa or L-DOPA (3,4-dihydroxy-L-phenylalanine) is an intermediate in dopamine biosynthesis. L-DOPA is used as a prodrug to increase dopamine levels for the treatment of Parkinson's disease, since it is able to cross the blood-brain barrier whereas dopamine itself cannot. Once L-DOPA has entered the central nervous system, it is metabolized to dopamine by aromatic L-amino acid decarboxylase [10,11]. The initial enzymatic reaction in the biosynthesis of brain catecholamines involves the formation of the catechol amino acid L-dihydroxyphenylalanine (L-DOPA) from tyrosine. Once formed, the L-DOPA is immediately decarboxylated to form dopamine, which in some neurons, is further transformed to norepinephrine [12]. L-DOPA can not be detected normally in the brain or in the blood [13], and thus it is unlikely that circulating L-DOPA is a physiological precursor for brain catecholamines. However, when exogenous L-DOPA is administered to experimental animals, the concentration of dopamine in the brain increases [14,15]. This observation, coupled with the finding that dopamine concentrations measured at autopsy in brains of patients with Parkinson's disease are low [16], suggested that exogenous L-DOPA might be useful in the treatment of Parkinsonism. That hypothesis has now been confirmed in numerous clinical studies [17-19].

As a part of our ongoing research work [20-24], here in the present communication we report the vibrational study carried out on tyrosine and L-DOPA. To the best of our knowledge neither the complete Raman and IR spectra nor the comparative quantum chemical calculations for tyrosine and L-DOPA have been reported so far in the literature. Therefore, the aim of this paper is to interpret theoretically calculated vibrational spectra of the two well known amino acids tyrosine and L-DOPA by means of the potential energy distribution (P.E.D.) analysis of all fundamental vibrational modes. In this regard, with the help of VEDA program both the P.E.D. analysis and its optimization were carried out [25]. Based on the DFT calculations we also interpreted the experimental IR and Raman spectra of these title compounds.

FT-IR and FT-Raman spectra

The FT-IR and FT-Raman spectra of tyrosine and L-DOPA were taken from the Sigma-Aldrich chemical company (USA) with a stated purity of greater than 99% in condensed phase [26-29]. The observed frequencies from FT-IR and FT-Raman spectra of tyrosine and L-DOPA are given in Table 2 and 3 respectively.

Computational Details

The entire calculations were performed on a Pentium IV/1.66 GHZ personal computer using Gaussian 03W [30] program package, invoking gradient geometry optimization [31]. Conformers are generated by Monte Carlo Multiple Minimum method [32] and these possible conformers of tyrosine are shown in Fig. 1.1-1.3 and of L-DOPA are shown in Fig.2.1-2.12. There are 3 possible conformer for tyrosine and 12 for L-DOPA. They were minimized without any constraint in the potential energy surface at B3LYP level, adopting the standard 6-311G(d,p) basis set. We can easily see that the second conformer of tyrosine (Fig.1.2) and fifth conformer of L-DOPA (Fig. 2.5) are most stable than other possible conformers as these two are having minimum energy. That's why all the calculations are performed on these two conformers. The optimized structural parameters were used in the vibrational frequency calculations to characterize all stationary points as minima. We have utilized the gradient corrected density functional theory (DFT) [33] with the three-parameter hybrid functional (B3LYP) [34] for the exchange part and the Lee-Yang-Parr (LYP) correlation function [35], for the computation of molecular structure, vibrational frequencies, and energies of the optimized structures. Density functional theory offers electron correlation which is frequently comparable to second-order Moller-Plesset theory (MP2) [36,37]. Vibrational frequencies calculated at B3LYP/6-311G(d,p) level were scaled by a factor of 0.96 [38]. Next, the spectra were analyzed in terms of the PED contributions by using the VEDA program [25]. Finally, the calculated normal mode vibrational frequencies also provided the thermodynamic properties through the principle of statistical mechanics.

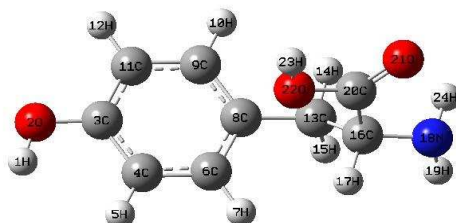


Fig. 1.1- 1st possible conformer of tyrosine with $E=-630.17207196$ a.u

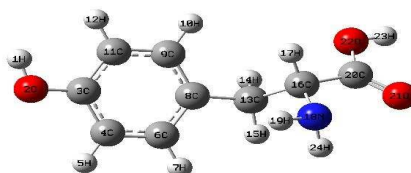


Fig. 1.2- 2nd possible conformer of tyrosine with $E=-630.17618551$ a.u

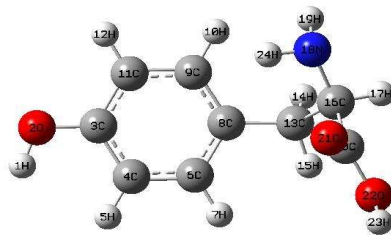


Fig. 1.3- 3rd possible conformer of tyrosine with E=-630.17087645 a.u

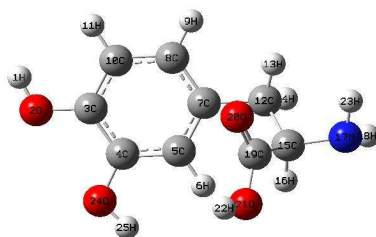


Fig. 2.1- 1st possible conformer of L-DOPA with E=-705.40778134 a.u

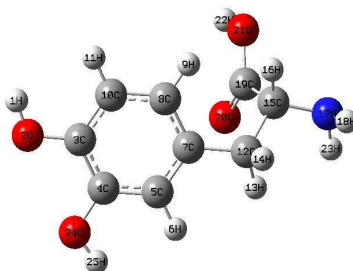


Fig. 2.2- 2nd possible conformer of L-DOPA with E=-705.40686372 a.u

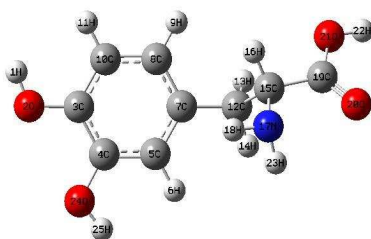


Fig. 2.3- 3rd possible conformer of L-DOPA with E=-705.41067308 a.u

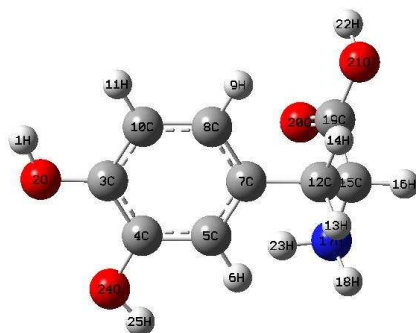


Fig. 2.4- 4th possible conformer of L-DOPA with E=-705.40268385 a.u

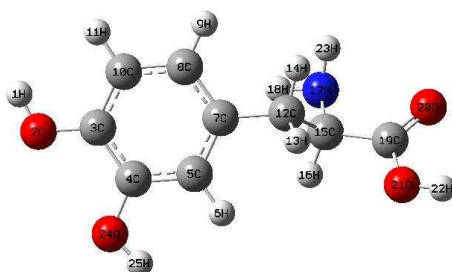


Fig. 2.5- 5th possible conformer of L-DOPA with E=-705.41091503 a.u

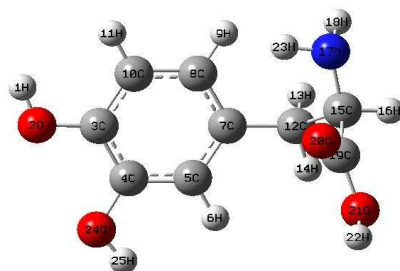


Fig. 2.6- 6th possible conformer of L-DOPA with E=-705.40297209 a.u

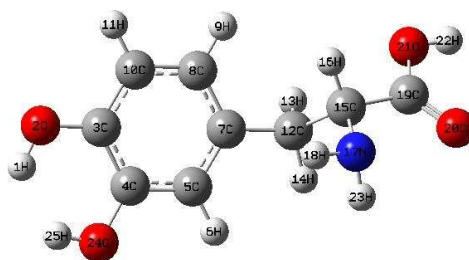


Fig. 2.7- 7th possible conformer of L-DOPA with E=-705.40760544 a.u

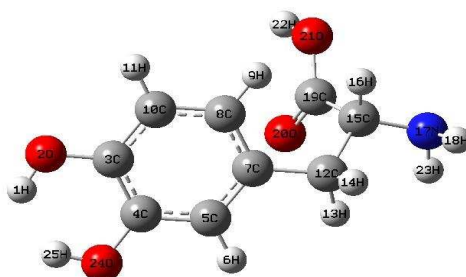


Fig. 2.8- 8th possible conformer of L-DOPA with E=-705.40358570 a.u

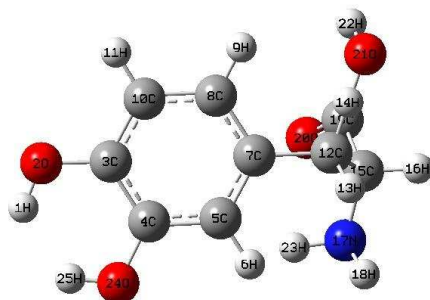


Fig. 2.9- 9th possible conformer of L-DOPA with $E=-705.40001278$ a.u

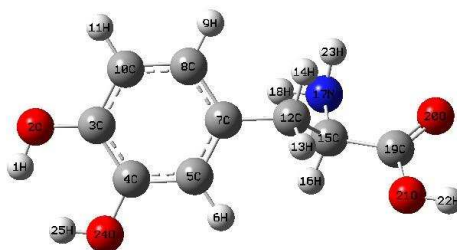


Fig. 2.10- 10th possible conformer of L-DOPA with $E=-705.40767017$ a.u

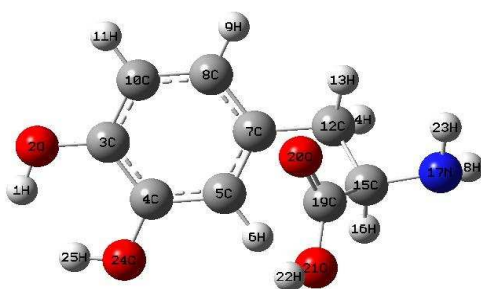


Fig. 2.11- 11th possible conformer of L-DOPA with $E=-705.40453203$ a.u

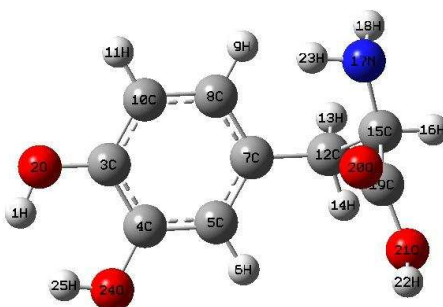


Fig. 2.12- 12th possible conformer of L-DOPA with $E=-705.39974548$ a.u

RESULT AND DISCUSSION

4.1. Molecular geometry

The optimized structural parameters of tyrosine and L-DOPA calculated by DFT, B3LYP method with the 6-311G(d,p) basis set are listed in Table 1 in accordance with the atom numbering scheme given in Fig. 1.2 and Fig. 2.5. For example in tyrosine, the optimized bond lengths of C-C in phenyl ring falls in the range from 1.390Å to 1.400Å, which are in good agreement with those of L-DOPA [1.385Å-1.415Å]. The optimized C8-C13 bond length is 1.500Å for tyrosine which is also in excellent agreement with C7-C12 bond length [1.510Å] for L-DOPA. The optimized C13-C16 bond length is 1.564Å for tyrosine, which is also in very good agreement with C12-C15 bond length [1.562Å] for L-DOPA. The optimized C-N bond length is 1.457Å for tyrosine, which is also in excellent agreement with C-N bond length [1.458Å] for L-DOPA. The optimized C=O bond length is 1.204Å for tyrosine, which is also in very good agreement with C=O bond length [1.201Å] for L-DOPA. The other calculated bond lengths and bond angles also shown an excellent agreement in tyrosine and L-DOPA.

4.2 Vibrational frequencies

The experimental frequencies from FT-IR and FT-Raman spectra of tyrosine and L-DOPA are given in Table 2-3. The descriptions concerning the assignment have also been in Table 2-3. VEDA Program [25] was used for P.E.D. analysis and to assign the calculated harmonic frequencies. Comparing the calculated frequencies in increasing order of frequencies of these two title compounds at B3LYP/6-311G(d,p) level, we can easily see that the calculated frequencies of tyrosine is greater than that of L-DOPA. While in decreasing order of frequencies, we can also see that most of the calculated frequencies of L-DOPA are greater than that of tyrosine.

Table 1: Optimized geometrical parameters of tyrosine and L-DOPA

S. No	Tyrosine Parameters	Calculated	L-Dopa Parameters	Calculated
	Bond lengths (Å)			
1	H1-O2	0.972	H1-O2	0.965
2	O2-C3	1.361	O2-C3	1.363
3	C3-C4	1.394	C3-C4	1.415
4	C3-C11	1.397	C3-C10	1.389
5	C4-H5	1.088		
6	C4-C6	1.390	C4-C5	1.385
7	C6-H7	1.082	C5-H6	1.088
8	C6-C8	1.399	C5-C7	1.401
9	C8-C9	1.400	C7-C8	1.394
10	C8-C13	1.500	C7-C12	1.510
11	C9-H10	1.083	C8-H9	1.085
12	C9-C11	1.390	C8-C10	1.396
13	C11-H12	1.083	C10-H11	1.084
14	C13-H14	1.096	C12-H13	1.095
15	C13-H15	1.094	C12-H14	1.095
16	C13-C16	1.564	C12-C15	1.562
17	C16-H17	1.092	C15-H16	1.093
18	C16-N18	1.457	C15-N17	1.458
19	C16-C20	1.521	C15-C19	1.517
20	N18-H19	1.013	N17-H18	1.016
21	N18-H24	1.017	N17-H23	1.018
22	C20=O21	1.204	C19=O20	1.201
23	C20-O22	1.358	C19-O21	1.355
24	O22-H23	0.970	O21-H22	0.969
25			C4-O24	1.386
26			O24-H25	0.964
	Bond Angles (degree)			
27	H1-O2-C3	109.4	H1-O2-C3	106.1
28	O2-C3-C4	122.8	O2-C3-C4	120.5
29	O2-C3-C11	117.3	O2-C3-C10	120.2
30	C4-C3-C11	119.9	C4-C3-C10	119.1
31	C3-C4-H5	120.1		
32	C3-C4-C6	120.4	C3-C4-C5	120.8
33	H5-C4-C6	120.0		
34	C4-C6-H7	119.2	C4-C5-H6	119.4
35	C4-C6-C8	121.4	C4-C5-C7	120.2
36	H7-C6-C8	119.6	H6-C5-C7	120.0
37	C6-C8-C9	117.8	C5-C7-C8	118.3
38	C6-C8-C13	121.9	C5-C7-C12	120.3
39	C9-C8-C13	120.5	C8-C7-C12	121.4
40	C8-C9-H10	119.7	C7-C8-H9	119.8
41	C8-C9-C11	121.8	C7-C8-C10	121.4
42	H10-C9-C11	120.0	H9-C8-C10	119.3
43	C3-C11-C9	119.9	C3-C10-C8	120.7
44	C3-C11-H12	118.7	C3-C10-H11	118.3
45	C9-C11-H12	121.0	C8-C10-H11	121.1
46	C8-C13-H14	110.5	C7-C12-H13	110.0
47	C8-C13-H15	110.2	C7-C12-H14	110.1
48	C8-C13-C16	112.6	C7-C12-C15	112.4
49	H14-C13-H15	107.2	H13-C12-H14	107.3
50	H14-C13-C16	108.6	H13-C12-C15	108.3
51	H15-C13-C16	108.4	H14-C12-C15	108.0

52	C13-C16-H17	107.7	C12-C15-H16	107.8
53	C13-C16-N18	116.1	C12-C15-N17	116.1
54	C13-C16-C20	108.0	C12-C15-C19	107.4
55	H17-C16-N18	108.4	H16-C15-N17	108.4
56	H17-C16-C20	105.3	H16-C15-C19	105.7
57			N17-C15-C19	110.3
58	C16-N18-H19	109.9	C15-N17-H18	109.9
59	C16-N18-H24	110.5	C15-N17-H23	110.4
60	H19-N18-H24	107.8	H18-N17-H23	108.1
61	C16-C20=O21	125.3	C15-C19=O20	125.4
62	C16-C20-O22	112.2	C15-C19-O21	112.0
63			O20=C19-O21	122.6
64	C20-O22-H23	106.8	C19-O21-H22	106.8
65			C3-C4-O24	114.5
66			C5-C4-O24	124.7
67			C4-O24-H25	110.6

Table 2: Vibrational wave numbers obtained for tyrosine at B3LYP/6-311G(d,p) in cm^{-1} , Experimental frequencies from FT-IR and FT-Raman spectra in cm^{-1} , IR intensities ($\text{K}_m \text{mol}^{-1}$), Raman scattering activities ($\text{\AA}^4 \text{amu}^{-1}$) and assignment with P.E.D. percentage in square brackets.

S. No	Wave Number Unscal. Scal.	Exp. Freq. I R (Raman)	IR Int.	Raman activity	Assignment [P.E.D]
1	35 34		3	0	$\tau(\text{CCCO})\text{adj N}[87]$
2	43 41		1	3	$\tau(\text{CCCO})\text{adj N}[72]+\tau(\text{CCCN})[12]$
3	59 57		1	2	$\tau(\text{CCCN})[66]+\tau(\text{CCCO})\text{adj N}[12]$
4	64 61		0	4	$\tau(\text{CCCC})\text{R}[51]+\phi(\text{CCC})\text{adj R}[28]$
5	164 157	(160)	1	2	$\phi(\text{CCC})\text{adj O}[57]$
6	186 179		2	1	$\tau(\text{CCCO})\text{R}[44]+\phi(\text{CCC})\text{adj R}[26]$
7	268 257	(255)	13	1	$\phi(\text{CCO})\text{adj N}[49]+\tau(\text{HNCC})\text{adj R}[23]$
8	292 280		7	2	$\phi(\text{CCC})\text{adj R}[47]+\tau(\text{HNCC})\text{adj R}[16]$
9	328 315		17	5	$\tau(\text{HNCC})\text{adj R}[53]+\phi(\text{CCO})\text{adj N}[26]$
10	344 330		109	7	$\tau(\text{HOCC})\text{R}[93]$
11	350 336	(338)	15	1	$\phi(\text{CCN})\text{adj R}[42]+\tau(\text{CCCO})\text{R}[16]+$ $\tau(\text{CCCC})\text{R}[11]$
12	393 377	(380)	5	8	$\phi(\text{CCN})\text{adj R}[16]+\phi(\text{HNC})[10]$
13	424 407		2	0	$\tau(\text{CCCC})\text{R}[76]+\phi(\text{CCO})\text{R}[12]$
14	431 414	(432)	8	1	$\phi(\text{CCO})\text{R}[72]+\tau(\text{CCCC})\text{R}[12]$
15	493 473	475	12	2	$\phi(\text{CCC})\text{R}[46]+\tau(\text{CCCC})\text{R}[19]$
16	529 508	495(495)	18	2	$\tau(\text{CCCC})\text{R}[30]$
17	556 534	535(530)	12	1	$\tau(\text{CCCC})\text{R}[28]$
18	599 575	578(575)	96	5	$\tau(\text{HOCC})\text{adj N}[72]$
19	632 607		39	4	$\phi(\text{CCN})\text{adj O}[61]$
20	658 632	652(645)	0	8	$\phi(\text{CCO})\text{R}[83]+\nu(\text{CC})\text{R}[12]$
21	720 691		10	4	$\tau(\text{CCCC})\text{R}[64]+\nu(\text{CC})\text{adj N}[11]$
22	749 719	717(716)	18	4	$\tau(\text{OCOC})[58]$
23	794 762	745(745)	34	15	$\nu(\text{CC})\text{R}[58]+\tau(\text{OCOC})[12]$
24	814 781	793	39	2	$\tau(\text{CCCH})\text{R}[81]$
25	828 795	(800)	109	6	$\tau(\text{HCCO})\text{R}[59]$
26	849 815		49	18	$\nu(\text{CC})\text{adj O}[54]+\phi(\text{HNH})[16]$
27	860 826	833(830)	76	6	$\phi(\text{HNH})[34]+\tau(\text{HCCO})\text{R}[16]+$ $\nu(\text{CC})\text{adj O}[12]$
28	877 842	844(848)	26	11	$\phi(\text{CCC})\text{adj N}[12]$
29	893 857	878(877)	28	8	$\nu(\text{CC})\text{adj O}[48]$
30	942 904	898(900)	3	1	$\tau(\text{HCCH})\text{R}[85]$

31	961	923	942	2	1	$\tau(\text{HCCC})\text{R}[91]$
32	1009	969	(945)	40	20	$\nu(\text{CC})\text{adj N}[30]$
33	1029	988	985(985)	3	1	$\phi(\text{CCC})\text{R}[85]$
34	1094	1050	1048(1047)	85	16	$\nu(\text{NC})[48]$
35	1120	1075	1100(1100)	34	2	$\phi(\text{HCC})\text{R}[34]+\nu(\text{CC})\text{R}[18]+$ $\phi(\text{HNC})[13]$
36	1146	1100	1110(1115)	112	8	$\phi(\text{HCC})\text{adj R}[39]+\nu(\text{CC})\text{adj O}[15]$
37	1194	1146	1157	184	4	$\nu(\text{CC})\text{R}[16]+\phi(\text{HNC})[11]$
38	1196	1148		13	2	$\phi(\text{HCC})\text{R}[61]+\nu(\text{CC})\text{R}[13]$
39	1206	1158	1178(1180)	41	10	$\phi(\text{HOC})\text{R}[44]+\nu(\text{CC})\text{adj O}[12]$
40	1224	1175	1200(1202)	2	23	$\nu(\text{CC})\text{adj R}[58]+\phi(\text{HCC})\text{R}[22]$
41	1260	1210	1218(1220)	49	3	$\phi(\text{HNC})[33]+\tau(\text{HCCC})\text{adj R}[24]$
42	1290	1238	1248	101	10	$\nu(\text{OC})\text{R}[68]+\phi(\text{HCC})\text{R}[13]$
43	1295	1243	(1250)	4	19	$\tau(\text{HCCC})\text{adj R}[57]+\phi(\text{HCC})\text{adj R}[11]$
44	1341	1287	1274(1270)	3	16	$\nu(\text{CC})\text{R}[23]+\tau(\text{HCCC})\text{adj R}[20]+$ $\phi(\text{HCC})\text{R}[16]$
45	1354	1300	(1288)	39	4	$\phi(\text{HOC})\text{adj N}[45]+\nu(\text{CC})\text{adj O}[24]+$ $\phi(\text{HCN})[15]$
46	1359	1305		8	18	$\tau(\text{HCCC})\text{adj R}[47]$
47	1365	1310	1333(1325)	34	2	$\phi(\text{HCC})\text{R}[44]+\nu(\text{CC})\text{R}[17]+$ $\phi(\text{HOC})\text{R}[16]$
48	1428	1371	1370(1370)	17	5	$\phi(\text{HCN})[55]+\phi(\text{HNC})[21]$
49	1470	1411	1419(1420)	23	1	$\nu(\text{CC})\text{R}[42]+\phi(\text{HCC})\text{R}[24]+$ $\phi(\text{HOC})\text{R}[11]$
50	1485	1426	1438(1435)	4	9	$\phi(\text{HCH})[83]+\tau(\text{HCCC})\text{adj R}[12]$
51	1545	1483	1458	116	2	$\phi(\text{HCC})\text{R}[45]+\nu(\text{CC})\text{adj R}[17]+$ $\nu(\text{CO})\text{R}[13]$
52	1631	1566	1518(1520)	17	10	$\nu(\text{CC})\text{R}[64]+\phi(\text{HCC})\text{R}[12]$
53	1655	1589	1593	25	2	$\phi(\text{HNH})[91]$
54	1656	1590	1608(1650)	46	59	$\nu(\text{CC})\text{R}[59]+\phi(\text{HCC})\text{R}[20]$
55	1834	1761	1900	309	9	$\nu(\text{C=O})[88]$
56	3025	2904		25	109	$\nu_s(\text{CH}_2)[98]$
57	3064	2941	2925(2930)	3	71	$\nu_{as}(\text{CH}_2)[95]$
58	3083	2960	2960(2970)	20	28	$\nu_{as}(\text{CH}_2)[96]$
59	3145	3019	(3015)	18	81	$\nu(\text{CH})\text{R}[91]$
60	3166	3039	3045(3048)	14	46	$\nu(\text{CH})\text{R}[87]$
61	3168	3041		8	129	$\nu(\text{CH})\text{R}[87]$
62	3198	3070	3205(3060)	9	146	$\nu(\text{CH})\text{R}[93]$
63	3495	3355		1	93	$\nu_s(\text{NH}_2)[100]$
64	3576	3433		8	41	$\nu_{as}(\text{NH}_2)[100]$
65	3758	3608		63	191	$\nu(\text{OH})\text{adj N}[100]$
66	3833	3680		68	139	$\nu(\text{OH})\text{R}[100]$

Unscal.: Unscaled; *Scal.:* Scaled; *v:* stretching; *vs:* symmetric stretching; *vas:* asymmetric stretching; ϕ : bending; τ : torsion; R: Ring; adj-adjacent.

Table 3: Vibrational wave numbers obtained for L-DOPA at B3LYP/6-311G(d,p) in cm^{-1} , Experimental frequencies from FT-IR and FT-Raman spectra in cm^{-1} , IR intensities ($\text{K}_m \text{mol}^{-1}$), Raman scattering activities ($\text{\AA}^4 \text{amu}^{-1}$) and assignment with P.E.D. percentage in square brackets.

S. No	Wave Number		Exp. Freq. I R (Raman)	IR Int.	Raman activity	Assignment [P.E.D]
	Unscal.	Scal.				
1	35	34		3	1	$\tau(\text{CCCO})\text{adj N}[73]$
2	44	42		2	2	$\tau(\text{CCCO})\text{adj N}[71]$
3	60	58		1	1	$\tau(\text{CCCO})\text{adj N}[69]$

4	66	63		1	3	$\tau(\text{CCCC})\text{R}[49]+\phi(\text{CCC})\text{adj N}[27]$
5	163	156	(140)	3	2	$\phi(\text{CCC})\text{adj O}[59]$
6	174	167	(173)	4	1	$\tau(\text{CCCO})\text{R}[33]+\phi(\text{CCC})\text{adj N}[16]+$ $\tau(\text{HOCC})\text{adj N}[12]$
7	218	209	(200)	140	3	$\tau(\text{HOCC})\text{R}[91]$
8	238	228		1	2	$\tau(\text{CCCO})\text{R}[55]$
9	267	256	(260)	13	2	$\phi(\text{CCO})\text{adj N}[45]+\phi(\text{CCC})\text{adj R}[17]$
10	292	280		8	1	$\phi(\text{CCC})\text{adj R}[37]+\tau(\text{HNCC})\text{adj}$ $\text{N}[22]$
11	312	299	(300)	6	2	$\phi(\text{CCO})\text{R}[86]$
12	323	310	(318)	23	3	$\tau(\text{HNCC})\text{adj R}[54]+\phi(\text{CCO})\text{adj}$ $\text{N}[26]$
13	361	347	(348)	10	2	$\phi(\text{CCN})\text{adj R}[35]+\tau(\text{CCCO})\text{R}[18]$
14	395	379	(366)	3	6	$\phi(\text{CCN})\text{adj R}[23]+\tau(\text{CCCO})\text{R}[18]$
15	433	416		68	1	$\tau(\text{HOCC})\text{R}[91]$
16	458	440		9	2	$\tau(\text{HOCC})\text{R}[58]+\phi(\text{CCC})\text{R}[23]$
17	467	448	463(465)	11	3	$\phi(\text{CCC})\text{R}[49]+\tau(\text{HOCC})\text{R}[22]$
18	520	499	475	2	9	$\phi(\text{CCO})\text{R}[49]$
19	538	516	528	7	2	$\phi(\text{CC=O})[49]+\nu(\text{NC})[14]$
20	590	566	555(553)	23	4	$\tau(\text{HOCC})\text{adj N}[44]+\phi(\text{CCO})\text{adj}$ $\text{N}[29]$
21	597	573		50	5	$\phi(\text{O=CO})[59]$
22	621	596	590(592)	73	0	$\tau(\text{HOCC})\text{adj N}[51]+\phi(\text{CCO})\text{adj}$ $\text{N}[11]$
23	654	628	615(614)	21	4	$\phi(\text{CCO})\text{adj N}[19]+\phi(\text{CC=O})[10]$
24	710	682	678(690)	3	4	$\tau(\text{CCCC})[72]$
25	736	707	725(720)	16	8	$\tau(\text{NCC=O})[38]$
26	775	744	738	5	5	$\nu(\text{CC})\text{adj N}[43]+\tau(\text{NCC=O})[22]$
27	806	774		28	31	$\nu(\text{CC})\text{R}[53]$
28	821	788	782(782)	99	7	$\tau(\text{HCCO})\text{R}[71]$
29	837	803	809	31	3	$\tau(\text{HCCO})\text{R}[78]$
30	854	820	822(814)	113	5	$\tau(\text{NHCH})[56]+\nu(\text{CC})\text{adj N}[14]$
31	876	841	845(845)	5	4	$\tau(\text{HCCO})\text{R}[29]$
32	888	852	868(870)	58	2	$\tau(\text{HCCC})\text{adj R}[28]+\tau(\text{NHCH})[21]$
33	936	899		5	1	$\tau(\text{HCCO})\text{R}[83]$
34	969	930	923(922)	37	4	$\nu(\text{CC})\text{adj R}[57]+\phi(\text{CCC})\text{R}[14]$
35	1015	974	988(986)	31	19	$\nu(\text{CC})\text{adj N}[33]$
36	1092	1048	1066(1065)	98	15	$\nu(\text{NC})[50]+\phi(\text{HNC})[13]+\phi(\text{HCN})[1$ $0]$
37	1123	1078		18	1	$\nu(\text{CC})\text{R}[19]+\phi(\text{HCC})\text{R}[18]+$ $\phi(\text{HCC})\text{adj N}[12]$
38	1133	1088	(1100)	234	8	$\nu(\text{CC})\text{adj O}[28]+\phi(\text{HCC})\text{R}[14]+$ $\phi(\text{HNC})[11]$
39	1164	1117	1122(1124)	19	4	$\phi(\text{HCC})\text{R}[36]+\nu(\text{CC})\text{R}[17]+$ $\phi(\text{HOC})\text{R}[10]$
40	1182	1135	1145(1142)	17	7	$\phi(\text{HOC})\text{R}[40]+\phi(\text{HCC})\text{adj N}[18]$
41	1200	1152	1160(1165)	99	9	$\phi(\text{HCC})\text{R}[28]+\phi(\text{HOC})\text{adj N}[17]+$ $\nu(\text{CC})\text{adj O}[12]$
42	1221	1172		55	16	$\phi(\text{HOC})\text{R}[32]+\phi(\text{HCC})\text{R}[25]$
43	1260	1210	1203	59	4	$\phi(\text{HNC})[19]+\phi(\text{HCC})\text{adj N}[12]+$ $\phi(\text{HCN})[10]$
44	1282	1231	1230	101	2	$\nu(\text{OC})\text{R}[38]+\phi(\text{CCC})\text{R}[28]+$ $\phi(\text{HCC})\text{adj N}[12]$
45	1299	1247		53	8	$\phi(\text{HCC})\text{adj N}[50]$
46	1310	1258	1255(1265)	136	24	$\nu(\text{CC})\text{R}[57]+\phi(\text{HCC})\text{R}[14]$

47	1341	1287	1285	7	36	$\tau(\text{HCCC})_{\text{adj R}}[54]$
48	1350	1296	1300(1300)	69	5	$\phi(\text{HOC})_{\text{adj N}}[46]+v(\text{CC})_{\text{adj O}}[17]+$ $\phi(\text{HCN})[12]$
49	1359	1305		16	10	$\phi(\text{HCC})_{\text{R}}[27]+\phi(\text{HOC})_{\text{R}}[14]+$ $\tau(\text{HCCC})_{\text{adj R}}[11]$
50	1411	1355	1352(1350)	29	15	$v(\text{CC})_{\text{R}}[36]+\phi(\text{HOC})_{\text{R}}[31]$
51	1426	1369		21	5	$\phi(\text{HCN})[49]+\phi(\text{HNC})[25]$
52	1474	1415	1405(1407)	95	4	$v(\text{CC})_{\text{R}}[52]+\phi(\text{HCC})_{\text{R}}[16]$
53	1491	1431	1460(1445)	9	9	$\phi(\text{HCH})[88]$
54	1558	1496	1500(1500)	136	5	$v(\text{CC})_{\text{R}}[53]+\phi(\text{HCC})_{\text{adj N}}[28]$
55	1647	1581	1572	27	6	$v(\text{CC})_{\text{R}}[64]$
56	1655	1589	1595	25	2	$\phi(\text{HNN})[92]$
57	1661	1595	1605(1610)	25	69	$v(\text{CC})_{\text{R}}[68]$
58	1830	1757		301	8	$v(\text{C=O})[88]$
59	3029	2908	2927	28	121	$v_{\text{s}}(\text{CH}_2)[98]$
60	3064	2941	(2933)	4	72	$v_{\text{as}}(\text{CH}_2)[95]$
61	3080	2957	2960(2980)	24	28	$v_{\text{as}}(\text{CH}_2)[96]$
62	3142	3016		17	66	$v(\text{CH})_{\text{R}}[97]$
63	3173	3046	(3038)	12	55	$v(\text{CH})_{\text{R}}[100]$
64	3190	3062	3072(3050)	5	152	$v(\text{CH})_{\text{R}}[100]$
65	3494	3354		2	95	$v_{\text{s}}(\text{NH}_2)[100]$
66	3576	3433		8	41	$v_{\text{as}}(\text{NH}_2)[100]$
67	3758	3608		71	196	$v(\text{OH})_{\text{adj N}}[100]$
68	3789	3637		105	85	$v(\text{OH})_{\text{R}}[100]$
69	3848	3694		75	102	$v(\text{OH})_{\text{R}}[100]$

Unscal.: Unscaled; Scal.: Scaled; v: stretching; vs: symmetric stretching; vas: asymmetric stretching; ϕ : bending; τ : torsion; R: Ring; adj-adjacent.

Table 4: Theoretically computed energies (a.u), zero-point vibrational energies (kcal mol⁻¹), rotational constants (GHz), entropies (Cal mol⁻¹ K⁻¹) and dipole moment (D) for Tyrosine and L-Dopa.

Parameters	Tyrosine	L-Dopa	
Total energy	-630.17618551	-705.41091503	
Zero-point energy	121.22195	123.89533	
Rotational Constants	2.37059	1.74391	
	0.34807	0.30353	
	0.31036	0.24353	
Entropy			
	Total	111.395	119.330
	Translational	41.404	42.850
	Rotational	30.508	31.077
Vibrational	39.483	45.403	
Dipole moment	3.348	2.289	

4.3 Vibrational assignment

Tyrosine has 24 atoms and 66 normal modes of fundamental vibration. All of the 66 fundamental vibrations are IR and Raman active. L-DOPA has 25 atoms and 69 normal modes of fundamental vibration. Here also all the 69 fundamental vibrations are IR and Raman active. Detailed description of vibrational modes can be given by means of normal coordinate analysis. The detailed vibrational assignments are achieved by comparing the band positions and intensities observed in FT-IR and FT-Raman spectra with wave numbers and intensities from molecular modeling calculations given in Table 2 and 3.

4.3.1 C-C Vibrations

For tyrosine, the C-C aromatic stretch known as semi-circle stretching predicted at 762, 857, 969, 1146, 1175, 1287, 1411, 1566 and 1590 cm^{-1} are in excellent agreement with experimental observations of both FT-IR and FT-Raman spectra with significant P.E.D. For L-DOPA, the C-C aromatic stretch known as semi-circle stretching predicted at 744, 930, 974, 1088, 1258, 1355, 1415, 1496, 1581 and 1595 cm^{-1} are also in good agreement with experimental observations of both FT-IR and FT-Raman spectra with significant P.E.D. The other C-C vibrations, like bending and torsional vibrations are also found in excellent agreement with experimental data with appropriate P.E.D., for both title compounds.

4.3.2 C-H Vibrations

The hetero aromatic structure shows the presence of C-H stretching vibration in the region 3000-3100 cm^{-1} , which is the characteristic region for the ready identification of C-H stretching vibration [39]. Accordingly in the present study for tyrosine, the C-H vibrations are calculated at 3019, 3039 and 3070 cm^{-1} respectively with significant P.E.D. and are supported by experimental data. While for L-DOPA, the C-H vibrations are calculated at 3046 and 3062 cm^{-1} respectively with appropriate P.E.D. and are supported excellently by experimental data.

4.3.3 O-H Vibrations

In a vibrational spectra, the strength of hydrogen bond determines the position of O-H band. Usually the O-H stretching appears at 3600-3400 cm^{-1} [40]. In this study tyrosine showed a very strong absorption peak at 3608 and 3680 cm^{-1} with P.E.D. [100], which are due to the O-H stretching vibration. While L-DOPA also showed very strong absorption peak at 3608, 3637 and 3694 cm^{-1} with same P.E.D., which are also due to the O-H stretching vibration. The different bending vibrations of the hydroxyl groups are also identified and they are listed in Table 2 and 3.

4.3.4 NH₂ group Vibrations

The scaled NH₂ asymmetric stretch is calculated at 3433 cm^{-1} for tyrosine and also at 3433 cm^{-1} for L-DOPA with P.E.D.[100]. Whereas NH₂ symmetric stretch is calculated at 3355 cm^{-1} for tyrosine and at 3354 cm^{-1} for L-DOPA with P.E.D.[100]. The various bending vibrations of NH₂ group for both title compounds are also found to be in good agreement with the experimental data with appropriate P.E.D.

4.3.5 Methylene group Vibrations

The asymmetric CH₂ stretching vibrations are generally observed in the region 3100-3000 cm^{-1} , while the symmetric stretch will appear between 3000-2900 cm^{-1} [41]. For tyrosine, the symmetric CH₂ stretching vibrations is calculated at 2904 cm^{-1} and asymmetric CH₂ stretching vibrations are calculated at 2941 and 2960 cm^{-1} with significant P.E.D. and are also supported by experimental data. For L-DOPA, the symmetric CH₂ stretching vibrations is calculated at 2908 cm^{-1} and the asymmetric CH₂ stretching vibrations are calculated at 2941 and 2957 cm^{-1} with appropriate P.E.D. and are also supported by experimental data. The various bending CH₂ vibrations are also found to be in excellent agreement with experimental data for both title compounds.

4.3.6 Carbonyl Absorption

Carbonyl absorptions are sensitive and both the carbon and oxygen atoms of the carbonyl group move during the vibration and they have nearly equal amplitude. In the present study the C=O stretching vibration is observed at 1761 cm^{-1} for tyrosine and at 1757 cm^{-1} for L-DOPA with significant P.E.D. and is also supported by experimental data and literature.

4.4 Other Molecular Properties

Several calculated thermodynamic parameters are presented in Table 4. The zero point vibrational energy (ZPVE) of tyrosine is less than the L-DOPA, but the difference seems to be insignificant. The total energies are found less in L-DOPA, in comparison to the tyrosine. The total, translational, rotational and vibrational entropy of tyrosine is less than that of L-DOPA at room temperature, but the difference are only marginal. Values of rotational constants and dipole moment are greater in tyrosine, than that of L-DOPA.

CONCLUSION

Attempts have been made in the present work for the proper frequency assignments for the compound tyrosine and L-DOPA from the FT-IR and FT-Raman spectra. The equilibrium geometries and harmonic frequencies of tyrosine and L-DOPA were determined and analysed at DFT level of theory utilizing 6-311G(d,p) basis set, giving allowance for the lone pairs through diffused functions. The vibrational frequency calculation proved that both structures are stable (no imaginary frequency). The difference between the observed and scaled wave numbers values of most of the fundamentals is very small. Any discrepancy noted between the observed and the calculated frequencies may be due to the fact that the calculations have been actually done on a single molecule in the gaseous state contrary to the experimental values recorded in the presence of intermolecular interactions. The potential energy distribution contribution to each of the observed frequency shows the reliability and accuracy of the normal mode analysis. Therefore, the assignments made at higher levels of theory with only reasonable deviations from the experimental values, seems to be correct.

Acknowledgement

The corresponding author (Neeraj Misra) is grateful to UGC (new Delhi) for providing the financial assistance.

REFERENCES

- [1] RJ Wurtman; MC Lewis. *Karger*, **1991**, 32, 94-109.
- [2] AJ Gelenberg et al. *J. Affec. Disord.*, **1990**, 19, 125-132.
- [3] W Romanowski; S Grabiec. *Acta Physiol. Pol.*, **1974**, 25, 127-134.
- [4] HR Lieberman; S Corkin; BJ Spring; RJ Wurtman; JH Growden. *Am. J. Clin. Nutr.*, **1985**, 42, 366-370.
- [5] LE Banderet; HR Lieberman. *Brain Res. Bull.*, **1989**, 22, 759-762.
- [6] AJ Gelenberg; CJ Gibson; JD Wojcik. *Psychopharmacol. Bull.*, **1982**, 18, 7-18.
- [7] JS Meyer et al. *J. Am. Geriatr Soc.*, **1977**, 7, 289-298.
- [8] KE Goodwill; C Sabatier; C Marks; R Raaq; PF Fitzpatrick; RC Stevens. *Nat. Struct. Biol.*, **1997**, 4(7), 578-585.
- [9] KE Goodwill; C Sabatier; RC Stevens. *Biochem.*, **1998**, 37(39), 13437-13445.
- [10] JH Waite et al. *J. Adhesion*, **2005**, 81, 1-21.
- [11] PB Messersmith et al. *Macromol.*, **2006**, 39, 1740-1748.
- [12] J Glowinski; RJ Baldessarini. *Pharmacol. Rev.*, **1966**, 18, 1201-1238.
- [13] AH Anton; DF Sayre. *J. Pharmacol. Exp. Ther.*, **1964**, 145, 326-336.
- [14] LJ Poirier; P Singh; TL Sourkes; R Boucher. *Brain Res.*, **1967**, 6, 654-666.
- [15] J Constantinidis; G Bartholini; R Tissot; A Pletscher. *Experientia*, **1968**, 24(2), 130-131.
- [16] H Ehringer; O Hornykiewicz. *Klin Wochenschr.*, **1960**, 38, 1236-1239.
- [17] GC Cotzias; PS Papavasiliou; R Gellene. *New Eng. J. Med.*, **1969**, 280(7), 337-345.

- [18] MD Yahr; RC Duvoisin; MM Hoehn; MJ Schear; RE Barrett. *Trans. Amer. Neurol. Ass.*, **1968**, 93, 56-63.
- [19] DB Calne; GM Stern; AS Spiers; DR Laurence. *Lancet.*, **1969**, 8, 973-976.
- [20] SA Siddiqui; A Dwivedi; N Misra; N Sundaraganesan. *Journal of Molecular Structure: THEOCHEM*, **2007**, 847, 101-102.
- [21] SA Siddiqui; A Dwivedi; PK Singh; T Hasan; S Jain; N Sundaraganesan; H Saleem; N Misra. *J. Theo. Comput. Chem.*, **2009**, 8(3), 433-450.
- [22] SA Siddiqui; A Dwivedi; A Pandey; PK Singh; T Hasan; S Jain; N Misra. *J. Comp. Chem. Jpn.*, **2009**, 8(2), 59-72.
- [23] SA Siddiqui; A Dwivedi; PK Singh; T Hasan; S Jain; O Prasad; N Misra. *J. Struct. Chem.*, **2009**, 50(3), 421-430.
- [24] A Dwivedi; SA Siddiqui; O Prasad; L Sinha; N Misra. *J. Appl. Spect.*, **2009**, 76(5), 659-665.
- [25] MH Jamroz. *Vibrational Energy Distribution Analysis, VEDA 4 program*, Warsaw, **2004**.
- [26] <http://www.sigmaaldrich.com/spectra/ftir/FTIR009043.PDF>
- [27] <http://www.sigmaaldrich.com/spectra/rair/RAIR014464.PDF>
- [28] <http://www.sigmaaldrich.com/spectra/ftir/FTIR001390.PDF>
- [29] <http://www.sigmaaldrich.com/spectra/rair/RAIR001911.PDF>
- [30] MJ Frisch et al. *Gaussian, Inc.*, Wallingford CT, **2004**.
- [31] HB Schlegel. *J. Comput. Chem.*, **1982**, 3, 214-218.
- [32] G Chang; WC Guida; WC Still. *J. Am. Chem. Soc.*, **1989**, 111, 4379-4386.
- [33] P Hohenberg; W Kohn. *Phys. Rev.*, **1964**, B136, 864-871.
- [34] AD Becke. *J. Chem. Phys.*, **1993**, 98, 5648-5652.
- [35] C Lee; W Yang; RG Parr. *Phys. Rev.*, **1988**, B37, 785-789.
- [36] N Sundaraganesan; H Saleem; S Mohan; M Ramalingam. *Spectrochim. Acta*, **2005**, A61, 377-385.
- [37] N Sundaraganesan; S Ilakiamani; H Saleem; PM Wojaechiwsju; D Michalska. *Spectrochim. Acta*, **2005**, A61, 2995-3001.
- [38] PL Fast; J Corchado; ML Sanches; DG Truhlar. *J. Phys. Chem.*, **1999**, A103, 3139-3143.
- [39] V Krishnakumar; RJ Xavier. *Ind. J. Pure Appl. Phys.*, **2003**, 41, 597-601.
- [40] V Krishnakumar; R Ramasamy. *Spectrochim. Acta*, **2005**, A61, 2526-2532.
- [41] V Krishnakumar; RJ Xavier; T Chithambarathanu. *Spectrochim. Acta*, **2005**, A62, 931-939.